Neurobiology of Disease

Large Soluble Oligomers of Amyloid β-Protein from Alzheimer Brain Are Far Less Neuroactive Than the Smaller Oligomers to Which They Dissociate

Ting Yang, Shaomin Li, ⬤Huixin Xu, Dominic M. Walsh, and Dennis J. Selkoe

Ann Romney Center for Neurologic Diseases, Department of Neurology, Brigham and Women's Hospital, Harvard Medical School, Boston, Massachusetts 02115

Soluble oligomers of amyloid β-protein (oAβ) isolated from the brains of Alzheimer's disease (AD) patients have been shown experimentally (in the absence of amyloid plaques) to impair hippocampal synaptic plasticity, decrease synapses, induce tau hyperphosphorylation and neuritic dystrophy, activate microglial inflammation, and impair memory in normal adult rodents. Nevertheless, there has been controversy about what types of oligomers actually confer these AD-like phenotypes. Here, we show that the vast majority of soluble Aβ species obtained from brains of humans who died with confirmed AD elute at high molecular weight (HMW) on nondenaturing size-exclusion chromatography. These species have little or no cytotoxic activity in several bioassays. However, incubation of HMW oAβ in mildly alkaline buffer led to their quantitative dissociation into low molecular weight oligomers (~8–70 kDa), and these were now far more bioactive: they impaired hippocampal LTP, decreased neuronal levels of β2-adrenergic receptors, and activated microglia in wt mice *in vivo*. Thus, most soluble Aβ assemblies in AD cortex are large and inactive but under certain circumstances can dissociate into smaller, highly bioactive species. Insoluble amyloid plaques likely sequester soluble HMW oligomers, limiting their potential to dissociate. We conclude that conditions that destabilize HMW oligomers or retard the sequestration of their smaller, more bioactive components are important drivers of Aβ toxicity. Selectively targeting these small, cytotoxic forms should be therapeutically beneficial.

Key words: β2-adrenergic receptor; Aβ aggregation; Alzheimer's; long-term potentiation; microglia activation; size-exclusion chromatography

---

Significance Statement

Oligomers of amyloid β-protein (oAβ) are tought to play an important role in Alzheimer's disease (AD), but there is confusion and controversy about what types and sizes of oligomers have disease-relevant activity. Using size-exclusion chromatography and three distinct measures of bioactivity, we show that the predominant forms of Aβ in aqueous extracts of AD brain are high molecular weight (HMW) and relatively inactive. Importantly, under certain conditions, the abundant HMW oAβ can dissociate into low molecular weight species, and these low molecular weight oligomers are significantly more bioactive on synapses and microglia than the HMW species from which they are derived. We conclude that conditions that destabilize HMW oAβ or retard the sequestration of smaller, more bioactive components are important drivers of Aβ toxicity.

Introduction

Converging lines of evidence support the concept that diffusible oligomers of the amyloid β-protein (Aβ) are the principal cytotoxic agents that induce a complex array of downstream effects

on neurons, microglia, astrocytes, and cerebral microvessels in Alzheimer's disease (AD) (Walsh and Selkoe, 2007). Because Aβ accumulation in the human brain occurs extracellularly for the most part, it is assumed that the soluble oligomers bind to the plasma membranes of these diverse cell types and trigger transmembrane signaling events that lead to the intracellular changes that occur in AD. Given the importance of this early triggering

Table 1. The epitopes of antihuman mouse IgG mAbs

Antibody	Species origins	Antigen	Epitope	Source
266	IgG1 mouse	Aβ (13–26)	Aβ (13–26)	Elan Pharmaceuticals
2G3	IgG2a mouse	Aβ (33–40)	Aβ 33–40 with free Val40	Elan Pharmaceuticals
21F12	IgG2a mouse	Aβ (33–42)	Aβ 33–42 with free Ile42	Elan Pharmaceuticals
3D6	IgG2b mouse	Aβ (1–5)	Aβ 1–5 with free Asp1	Elan Pharmaceuticals
1C22	Mouse	Aggregated (Aβ (1–40) S26C)2	Aβ oligomers	D.M.W. laboratory
6E10	IgG1 Mouse	Aβ (1–16)	Aβ (3–8)	Biolegend

action in AD pathogenesis, one needs to understand the characteristics of those oligomers that are most bioactive. This unresolved question has direct implications for selecting the most efficacious anti-Aβ therapeutic agents.

Soluble Aβ oligomers of a wide range of sizes appear to be in a complex equilibrium with the 8 nm fibrils of Aβ that are deposited in insoluble amyloid plaques. There has been considerable debate about which Aβ assemblies are most responsible for inducing cytotoxicity. The vast majority of studies attempting to address the bioactive properties of Aβ oligomers have used synthetic assemblies of one defined peptide length that are aggregated *in vitro* and applied under nonphysiological concentrations and conditions. In contrast, we have focused our work on the analysis of natural, aqueously soluble oligomers extracted directly from the affected cerebral cortex of patients with clinically and neuropathologically confirmed AD. Here, we use nondenaturing gel filtration to separate various sizes of soluble assemblies and assess their relative potencies in perturbing both synaptic and microglial function in normal rodent hippocampus. We find that the great majority of aqueously extractable oligomers are large in size and generally have very low bioactivity on the hippocampus, both *in vitro* and *in vivo*. However, if these large assemblies are first incubated in mildly alkaline aqueous buffer for 1–2 d, they dissociate in considerable part to smaller oligomers that are much more bioactive and can inhibit synaptic plasticity, alter cell-surface receptor levels, and induce a microglial inflammatory response. The demonstration of this equilibrium between large, relatively inactive assemblies and small, potently cytotoxic oligomers from human brain has implications for the role of amyloid plaques in the pathogenesis of cellular dysfunction in AD.

Materials and Methods

Human brain homogenates. Frozen cerebral cortices (stored at −80°C) were provided by Dr. M. Frosch (Massachusetts ADRC Neuropathology Core, Massachusetts General Hospital, Boston) under institutional review board-approved protocols. Frozen samples of temporal or frontal cortex (1 g) were allowed to thaw on ice, chopped into small pieces with a razor blade, and then homogenized with 25 strokes of a Dounce homogenizer (Fisher) in 4 ml ice-cold 20 mM Tris HCl, pH 7.4, containing 150 mM NaCl (TBS) and protease inhibitors. This TBS-soluble Aβ was separated from membrane-bound and plaque Aβ by centrifuging TBS homogenates at 175,000 × g at 4°C in a TLA 100 rotor (Beckman Coulter) for 30 min, and the supernatant (referred to as the TBS extract) was aliquoted and stored at −80°C. In general, the terms "soluble Aβ" and "aqueous extract" used herein refer to any forms of Aβ that remain in this supernatant following ultracentrifugation.

Antibodies and immunoassays. Immunoassays for Aβ1-x, Aβx-40, and Aβx-42 were performed on the MesoScale Discovery (MSD) platform as described previously (Yang et al., 2013, 2015). Monoclonal antibody (mAb) m266, which recognizes an epitope within Aβ13–26, was used for capture, and Asp1 (3D6), Aβ40 (2G3), or Aβ42 (21F12) specific antibodies were used for detection (Table 1). All samples and standards were analyzed in duplicate.

Oligomeric forms of Aβ were captured using our oligomer-preferring mAb, 1C22, and detected using biotinylated 3D6 (Yang et al., 2015).

Standard curves were generated with wild-type (wt) synthetic human Aβ1–40 for the Aβ1-x and Aβx-40 assays, and wt synthetic Aβ1–42 for the Aβx-42 assay. Amyloid-derived diffusible ligands were prepared from synthetic Aβ1–42, and size-exclusion chromatography (SEC) was used to isolate the high molecular weight (HMW) component, which served as the calibrant for the oligomer assay (Yang et al., 2015).

SEC. Whole TBS extracts (250 μl) or their void volume SEC fractions (500 μl) were injected onto either a Superdex 75 (10/30HR) column or a Superdex 200 (10/300GL) column (GE Healthcare) and eluted at a flow rate of 0.8 ml/min with 50 mM ammonium acetate, pH 8.5. The 1 ml fractions were collected; 0.5 ml of this material was used for ELISA, and the other 0.5 ml was lyophilized and used for Western blotting (Shankar et al., 2011). Samples were electrophoresed on 26-well, 4%–12% polyacrylamide Bis-Tris gels using MES running buffer (Invitrogen), and proteins were transferred to 0.2 μm nitrocellulose filters, the filters microwaved, and Aβ detected using a mixture of mAbs 2G3,21F12 (each at 1 μg/ml) and 0.5 μg/ml of mAb 6E10 (Table 1). Membranes were rinsed and incubated for 1 h with fluorescein-conjugated goat anti-rabbit or anti-mouse IgG (1:5,000; Invitrogen), and bands visualized using a LiCor Odyssey Infrared System.

Preparation of preincubation and postincubation samples. AD TBS extracts were prepared as described above and stored as 1 ml aliquots at −80°C. To generate postincubation samples, aliquots were thawed and chromatographed on a Superdex 75 10/30HR column eluted with 50 mM ammonium acetate, pH 8.5, and fractions 6 and 7 were pooled and incubated in sealed tubes at 37°C for 2 d. At the end of this period, these "postincubated samples" were used immediately or stored on ice and used within 6 h. "Preincubated samples" were produced exactly 2 d after the initiation of the 37°C incubation used to generate the postincubation samples: a 1 ml aliquot of AD-TBS extract was thawed and chromatographed just as described above. Fractions 6 and 7 of this SEC run were pooled and used immediately or stored on ice and then used within 6 h. In this way, both the "pre" and "post" samples were available for use and analysis at exactly the same time. For each experiment described in Results, we compared two or more matched pairs of preincubation and postincubation samples in the various bioassays.

Mice. All experiments involving mice were approved by the Harvard Medical School Committee on Animals. Both male and female C57BL/6 mice were used. Animals were housed in a temperature-controlled room on a 12 h light/12 h dark cycle and had free access to food and water.

Hippocampal slice preparation and electrophysiological recordings. Hippocampal slices were prepared and used as previously described (Li et al., 2013). Briefly, 350-μm-thick transverse slices from hippocampus of 6- to 8-week-old C57BL/6 mice were incubated for >90 min in aCSF containing the following (in mM): 124 NaCl, 2 KCl, 2 MgSO$_4$, 1.25 NaH$_2$PO$_4$, 2.5 CaCl$_2$, 26 NaHCO$_3$, 10 D-glucose, pH 7.4, 310 mOsm. Then slices were submerged beneath continuously perfused aCSF saturated with 95% O$_2$/5% CO$_2$. The 1 ml aliquots of an SEC fraction were added to the 9 ml of aCSF to yield a final volume of 10 ml of the slice perfusate for the LTP recordings. A stimulating electrode was placed in the Schaffer collaterals to deliver test and conditioning stimuli, and a borosilicate glass recording electrode filled with aCSF was positioned 200–300 μm from the stimulating electrode to record field EPSP in the stratum radiatum of CA1 (Li et al., 2013). A protocol that induces LTP lasting ~1.5 h in wt mice of this genetic background (two consecutive trains 1 s of stimuli at 100 Hz separated by 20 s) was used. Field potentials were amplified 100× using a Molecular Devices 200B amplifier and digitized with Digidata 1322A.

Table 2. Aβ oligomer levels are markedly elevated in aqueous extracts of brains from subjects with AD[a]

Case No.	NPDx	Sex	Age (yr)	Postmortem interval	Aβ oligomers ELISA (pg/ml)	Aβ1-x ELISA (pg/ml)
Control 1	Control	Male	92	12	0	107 ± 5
Control 2	Leukodystrophy	Female	34	<14	0	99 ± 11
Control 3	Control	Male	69	24	857 ± 62	75 ± 7
Control 4	Control	Female	79	NA	3084 ± 65	532 ± 36
Control 5	Control	Female	60	15	0	69 ± 28
AD1	AD	Female	70	7	9,052,737 ± 274	1982 ± 11
AD2	AD	Female	91	NA	450,728 ± 530	91 ± 22
AD3	AD	Male	81	20	218,257 ± 8923	257 ± 31
AD4	AD	Male	78	6	3,182,768 ± 433	1009 ± 21
AD5	AD	Male	86	<24	298,979 ± 347	112 ± 21
AD6	AD	Male	83	7	2,698,912 ± 527	292 ± 7

[a]Aqueous extracts were prepared from the brains of subjects with or without neuropathologically confirmed AD and analyzed using the monomer-preferring Aβ1-x immunoassay and the 1C22–3D6 oligomer-preferring immunoassay. NPDx, Neuropathological diagnosis. $n = 2$ for ELISAs (mean ± SD). NA, not available.

Data were sampled at 10 kHz and filtered at 2 kHz. Traces were obtained by pClamp 9.2 and analyzed using the Clampfit 9.2.

Hippocampal slices and measurement of β2AR. Hippocampal slices were sectioned by vibratome at 350 μm thickness and then treated under different conditions ($n = 3$ slices per treatment). Slices were collected in ice-cold TBS plus protease inhibitors and then homogenized with polypropylene pestle in 1.5 ml microcentrifuge tubes at least 20 passes. After nutating on ice for 10 min, the homogenate was passed through a 27G needle 4 times and then centrifuged at $1000 \times g$ for 10 min to remove nuclei and incompletely homogenized material (P1). The resulting supernatant (S1) was spun at $50,000 \times g$ for 1 h to obtain a P2 pellet. The supernatant (S2) was defined as the cytosolic fraction. The P2 was subsequently resuspended in TBS plus 1% Triton X-100 with protease inhibitors and homogenized again with a polypropylene pestle. The suspension was incubated at 4°C for 1 h and then spun at $50,000 \times g$ for 1 h to obtain the supernatant (S3), which included synaptosomes. Protein concentrations were determined using the BCA assay. We loaded 20 μg of total protein in each lane, separated on 4%–12% SDS-PAGE, and blotted onto nitrocellulose. The blot was blocked for 1 h at room temperature, followed by incubation overnight at 4°C with antibodies to β2-adrenergic receptor (Thermo Scientific) or transferrin receptor (Invitrogen). Membranes were rinsed and incubated for 1 h with goat anti-rabbit or mouse IgG (1:10,000; Invitrogen). Blots were scanned and imaged using a Li-Cor Odyssey system.

Synthetic Aβ40(S26C)$_2$ dimers, which readily form bioactive assemblies that alter β2AR expression (Li et al., 2013), were prepared as described previously (O'Nuallain et al., 2010) and used as a positive control to treat slices.

Immunohistochemistry and image analysis. Mice were killed and perfused first with 10 ml ice-cold HBSS and then 10 ml ice-cold 4% PFA. Brains were rapidly removed and immersed in 4% PFA for 2 h at 4°C, and then transferred to 30% sucrose solution for 48 h. The brains were cut into desired blocks and embedded in OCT, and 14 μm cryostat coronal sections were prepared. For immunofluorescence imaging, the sections were incubated with primary antibody (anti-p2ry12 1:500, gift of O. Butovsky, Brigham and Women's Hospital; anti-CD68 1:200, Abcam Ab53444). All images were obtained on a Zeiss LSM 510 confocal microscope with 20×/0.75 objective. Images obtained for the cell morphology analysis were set at 1024 × 1024 pixels and collected in Z stacks for 3D reconstruction. Image analysis was completed in ImageJ. Individual microglia images were selected and isolated manually, converted to binary images, then skeletonized for skeleton analysis or analyzed as a particle for circularity ($4\pi \times$ [Area]/[Perimeter]^2), solidity ([Area]/[Convex Area]) and %CD68/microglia (see Results).

Stereotactic intracerebroventricular injection and assessment of microglial activation. Mice were anesthetized with isoflurane and placed into a stereotactic frame with isoflurane vaporizer attached. The lateral ventricle was located as bregma −2.5 mm; midline 3.1 mm; dura −3.7 mm, and samples (4 μl each) were injected at a rate of ∼0.8 μl/min using a 25 μl airtight glass Hamilton syringe.

Results

The large majority of Aβ species found in aqueous extracts of AD brain are HMW but can be dissociated into small oligomers and monomers

TBS extracts were prepared from the frontal cortices of 6 neuropathologically confirmed late-onset AD patients and 5 non-AD control subjects (Table 2). Extracts were analyzed using Aβ monomer- and oligomer-preferring immunoassays and by SEC/Western blotting. Our MSD Aβ "1-x" assay uses mAbs 266 for capture and 3D6 for detection and has a lower limit of quantification of ∼16.4 pg/ml and preferentially recognizes Aβ monomers (Mably et al., 2015), whereas our MSD oAβ assay uses the oligomer-preferring mAb 1C22 for capture and then 3D6 for detection and preferentially recognizes Aβ oligomers, with a lower limit of quantification for amyloid-derived diffusible ligands (synthetic Aβ42 aggregates or ADDLs) of ∼18.7 pg/ml (Yang et al., 2015) (Table 2). Brain extracts from AD cases tended to have higher levels of Aβ1-x monomer than controls (e.g., average values of ∼835 pg/ml vs ∼170 pg/ml), but there was overlap, with some control brain extracts having higher monomer levels than certain AD cases. In contrast, oligomer levels measured using the 1C22–3D6 assay were always markedly higher in AD extracts than in extracts from aged control brains (e.g., average values of 3,226,123 pg/ml vs 788 pg/ml). Strikingly, no Aβ oligomers were detected in 3 of the 5 control extracts (Table 2). Thus, as we have documented previously, aqueous extracts of AD brain contain much higher levels of Aβ oligomers than extracts from non-AD brain (Xia et al., 2009; Yang et al., 2013, 2015), and within AD brains, the mean levels of oligomers far exceed those of monomers (e.g., 3,226,123 pg/ml vs 835 pg/ml).

Because the MSD immunoassays are at least 2 orders of magnitude more sensitive than our Western blotting protocol and the control brains contained only low levels of immunoassay-detectable Aβ, it was not surprising that Western blots of SEC fractions from all control brains failed to detect Aβ (for a representative Western blot of a control case, see Fig. 1A, left). However, Western blotting of SEC fractions of AD brain extracts, which contained nanogram per milliliter levels of MSD-detectable oAβ, revealed the presence of HMW Aβ species that eluted in and near the void volume of a Superdex 75 column (i.e., in fractions 6–8) (Fig. 1A). The Western blot-detectable Aβ in the void volume fractions migrated after denaturing SDS-PAGE as 2 bands: one centered at ∼4 kDa and the other centered at ∼7.5 kDa. These results indicate that the major Aβ species detected in AD extracts are HMW (≥150 kDa) but are SDS-labile
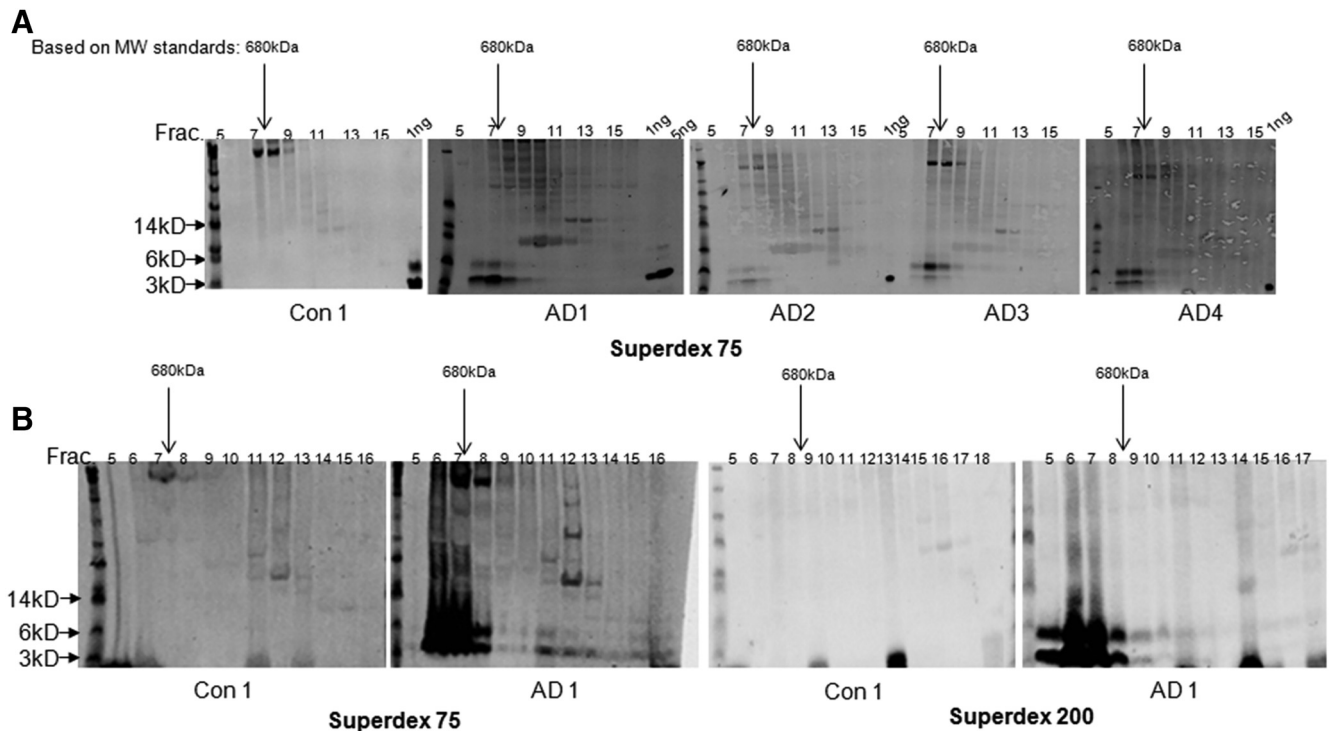
Figure 1. The large majority of Aβ in brain extracts elutes in or near the void volumes upon SEC using Superdex 75 and Superdex 200. *A*, Human brain extracts (200 μl) were chromatographed on a Superdex 75 column, fractions collected, lyophilized, and used for Western blotting with a mix of 2G3, 21F12, and 6E10. The major Aβ-immunoreactive species detected in all 4 AD brain extracts migrated on SDS-PAGE at ∼4 and ∼7.5 kDa and were most abundant in SEC fractions within or near the void volume of the Superdex 75 column. *B*, The elution of Aβ species on Superdex 75 versus Superdex 200 was compared by chromatographing aliquots of the same AD sample on the 2 different columns. The majority of the ∼4 and ∼7.5 kDa species eluted from both the Superdex 75 and Superdex 200 columns in or near the void. *A*, *B*, A ladder of MW standards is shown on the left of each gel. Arrows indicate the 14, 6, and 3 kDa standards. The SEC fraction numbers and the position and quantity of 1 ng, 5 ng synthetic Aβ1– 40 standards are indicated at the top of the gels. Arrow indicates the elution of a 680 kDa marker protein from SEC.

Table 3. Fraction numbers for elution of AD brain Aβ on two SEC columns

SEC column	Predicted (kDa)	Typical HMW oAβ-containing fractions	Typical monomer fractions
Superdex 75	3–70	6 – 8	11–13
Superdex 200	10 – 600	5 – 9	13–14

Table 4. Volumes and fraction numbers for elution of linear Dextran standards on Superdex 75

Dextran standards on Superdex 75	Eluted volume (ml)	Fraction no.
MW >1 mDa	8.16	6
MW 80 kDa	8.63	7
MW 25 kDa	9.97	8
MW 12 kDa	12.25	10
MW 5 kDa	14.21	12
MW 1 kDa	15.99	14

and, upon denaturing SDS-PAGE, break down to Aβ monomers and what appear to be SDS-stable dimers (McDonald et al., 2015).

In an effort to further characterize the approximate size range of the HMW soluble oAβ species, we performed SEC using a separation matrix (Superdex 200) that is better able to fractionate higher molecular weight material than is Superdex 75 (Tables 3, 4). Specifically, the manufacturer-reported exclusion limit of Superdex 75 is ∼75 kDa for globular proteins, whereas the analogous exclusion limit for Superdex 200 is ∼600 kDa. When extracts from brain AD1 were chromatographed on a Superdex 200 column, the vast majority of Aβ eluted in and near the void volume (Fig. 1B). These data indi-

cate that the major portion of Aβ extracted in physiological buffer from AD cortex consists of very large but still soluble aggregates spanning a mass range from ∼150 kDa to >600 kDa.

Our earlier work had suggested that the bioactivity of HMW oAβ assemblies and of washed amyloid plaque cores from AD brain tissue was low, and that only oligomer/dimer-rich low molecular weight (LMW) SEC fractions from AD brains consistently impaired synaptic plasticity (Shankar et al., 2008). We therefore examined the potential for disassembling the HMW oAβ species through dilution and incubation in the mildly alkaline buffer (50 mM ammonium acetate) used to elute them from the SEC columns. TBS extract of brain AD1 was chromatographed on a Superdex 75 column and 1 ml fractions collected. A portion of each fraction was lyophilized and analyzed by Western blot (Fig. 2A, left). The remainder of fraction 6 (void volume) was incubated at 37°C for 2 d. After incubation, fraction 6 was rechromatographed on the same Superdex 75 column (after thorough column washing) (Shankar et al., 2011), and the resultant fractions were collected and analyzed by Western blot. After the 2 d incubation, the Aβ that had originally eluted in the void of the first SEC (fraction 6; Fig. 2A, left) had dissociated to lower MW species (fractions 7–14; Fig. 2A, right). There was now relatively little oAβ in the void volume fraction, and most Aβ was detected in fractions 11–14, where synthetic Aβ dimers and monomers are known to elute (O'Malley et al., 2014; McDonald et al., 2015). ELISA analysis of the individual fractions of the first and second SEC runs produced results that paralleled those obtained by Western blotting (compare Fig. 2A,B). Specifically, when fractions of the first SEC of AD TBS extract were quantified with the
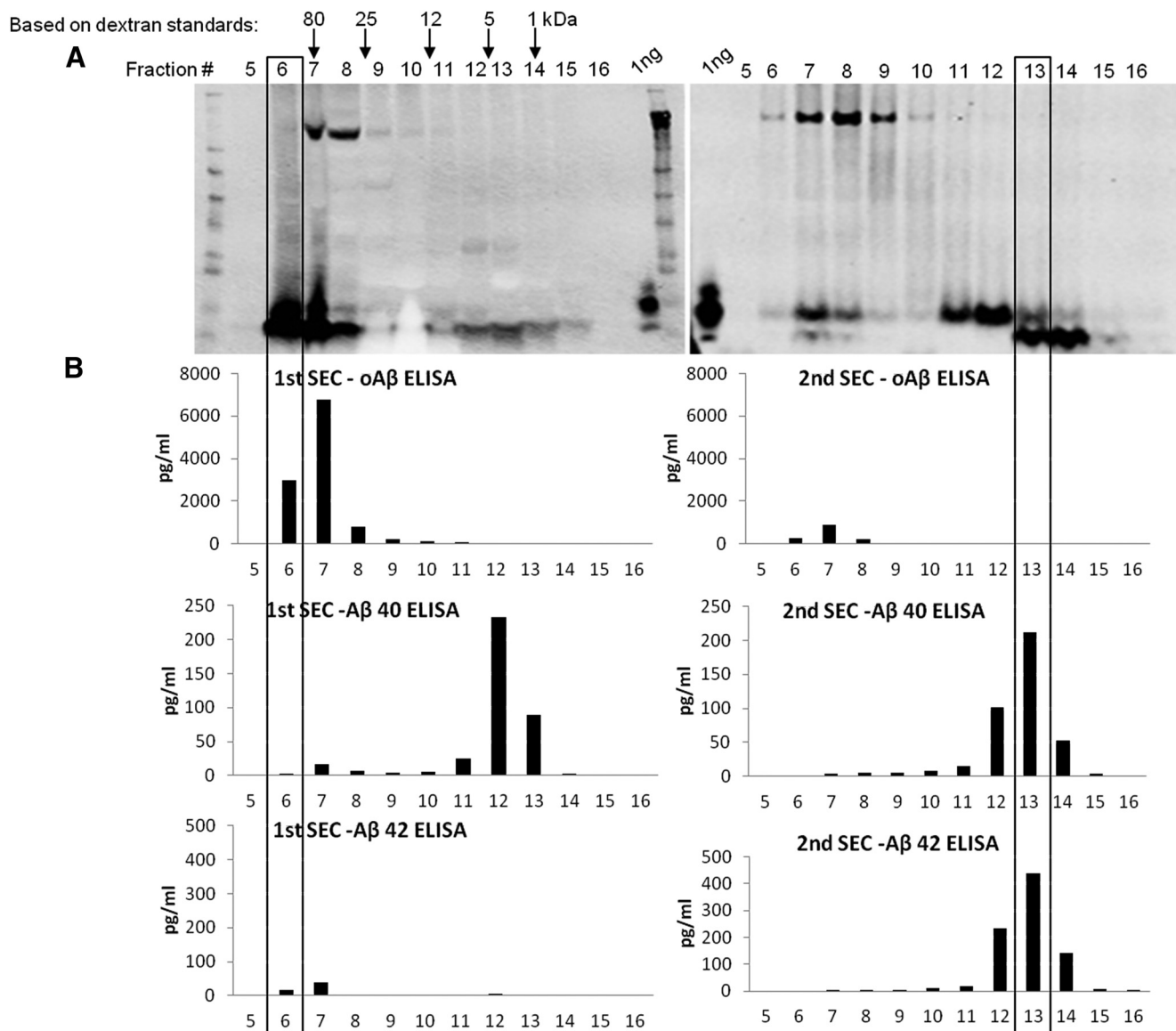
Figure 2. Incubation of soluble HMW oAβ isolated from human brain by SEC releases lower MW Aβ species. A TBS extract of brain AD1 was chromatographed on a Superdex 75 column, fractions were collected, and a portion of each analyzed by Western blot (mAbs 2G3 + 21F12 + 6E10) (**A**, left) and by ELISAs (**B**, left). Fraction 6 from the first SEC (boxed) was incubated at 37°C for 2 d and then chromatographed, and the resultant fractions analyzed by Western blot (2G3 + 21F12 + 6E10) (**A**, right) and by ELISAs (**B**, right), just as in the parent sample.

oAssay, nanogram levels of Aβ were detected in fractions 6 and 7, whereas <50 pg of Aβ was detected when fractions 6 and 7 were analyzed using the monomer-preferring Aβ x-40 and x-42 assays (Fig. 2B, left panels). The x-40 assay (but not the x-42 assay) also detected small quantities of Aβ in fractions where Aβ monomer is expected to elute (i.e., fractions 11–13). These results are entirely consistent with our quantitative analysis of the whole AD-TBS starting extracts (Table 2) and demonstrate that soluble AD brain extracts contain large amounts of HMW oligomers and only small amounts of Aβ monomer, the latter of which appears to terminate largely at Val40, given the specificity of mAb 2G3.

Importantly, when fraction 6 of Case AD 1 (Fig. 2A,B, left panels) was analyzed by the oAssay before versus after a 2 d *in vitro* incubation, the oligomer signal fell from 10,986 pg/ml to just 1401 pg/ml, whereas the x-42 monomer signal increased from 68 pg/ml before to 859 pg/ml after incubation (Table 5). These results indicate that incubation of AD brain-derived oligomers in mildly alkaline SEC buffer leads to almost complete

Table 5. The levels of Aβ oligomers decrease, whereas those of Aβ monomers increase, when the void volume fraction of AD brain is incubated at 37°C[a]

	Void volume preincubation			Void volume postincubation		
	x-40	x-42	Oligomers	x-40	x-42	Oligomers
AD1	388	68	10,986	407	859	1401
AD2	105	249	2079	823	4017	29
AD3	165	59	984	771	104	71
AD4	19	57	9711	745	1993	39

[a]SEC void volume fractions from 4 AD brains were analyzed using x-40 and x-42 monomer-preferring immunoassays, and the 1C22-3D6 oligomer-preferring immunoassay before and after 2 d incubation at 37°C.

dissociation of HMW oligomers and the simultaneous appearance of large amounts of Aβ monomer. A second SEC/ELISA analysis of the 2 d-incubated void volume fraction confirmed the results seen with the unfractionated incubated sample (compare Fig. 2A,B, right panels; Table 5); that is, the sample now contained little HMW Aβ, with the majority of Aβ now eluting in a manner consistent with Aβ monomers and dimers (fractions 11–

14) (Fig. 2 A, B, right panels). Of interest, the abundant SDS-stable dimers observed in fractions 10 and 11 by Western blot (Fig. 2A, right) were not well detected by the oAssay or the x-40/42 assays (Fig. 2B, right graphs). This was true regardless of which antibodies we used to construct an oAssay: 1C22, NAB61, or 3D6 for capture, and 3D6, 82E1, or 4G8, respectively, as detector (data not shown). Thus, certain LMW/dimeric oAβ species are poorly or not detected by oAssays that we had developed and standardized to detect HMW soluble oligomers. Similarly, they were poorly detected by our monomer assays.

As described above for AD1, the TBS extracts of all 4 of our initial AD brains were injected onto Superdex 75 columns, and the void volume fractions obtained were analyzed by ELISAs to quantify x-40, x-42, and oAβ (Table 5). The void volume fractions of all 4 AD brains behaved similarly, with incubation of AD brain-derived HMW oligomers in mildly alkaline buffer causing almost complete dissociation of HMW oligomers and the simultaneous appearance of large amounts of Aβ monomers and dimers. We compared the effects of incubating the initial void volume fraction of AD2 for 6 h versus 24 h versus 48 h, and the longer incubations led to much more HMW oAβ dissociation to LMW species, as expected (Fig. 3). For subsequent experiments aimed at investigating the bioactivity of the HMW versus dissociated Aβ species, we set our void volume incubation protocol as a 37°C incubation in 50 mM ammonium acetate, pH 8.5, for 2 d.

LMW Aβ postincubation is more bioactive than fresh HMW Aβ in inhibiting hippocampal synaptic plasticity

We next asked which Aβ assemblies (the original HMW oAβ species or the LMW oligomers/dimers dissociated from them) are more active in inhibiting synaptic function in the hippocampus, as judged by quantifying the degree of LTP, a widely validated electrophysiological correlate of learning and memory. We applied matched preincubation and postincubation samples of the HMW SEC fractions (fractions 6 and 7) of TBS extracts from each of six AD brains. Using the HMW SEC fraction of Case AD1, both the fresh and postincubation samples depressed LTP, but only the postincubation sample exerted a significant effect (preincubation: $140 \pm 6\%$, $n = 8$, vs postincubation: $121 \pm 4\%$, $n = 10$; $p < 0.001$) (Fig. 4A). The LTP value for the preincubation sample was not significantly different from plain aCSF buffer ($155 \pm 6\%$, $n = 6$) used on adjacent slices in the same experiment. When HMW SEC fractions (fractions 6 and 7) of the second brain (AD2) were tested, the preincubation sample had no significant effect on LTP versus aCSF vehicle alone (preincubation: $167 \pm 13\%$, $n = 6$, vs aCSF $172 \pm 5\%$, $n = 7$; $p > 0.05$), whereas the postincubation sample significantly inhibited LTP ($141 \pm 5\%$, $n = 7$; $p < 0.01$) (Fig. 4B). Similar results were obtained when HMW SEC fractions 6 and 7 of TBS extracts AD3, AD4, AD5, and AD6 were tested: postincubation samples caused more significant LTP depression than their matched preincubation samples (AD3: pre: $137 \pm 6\%$, $n = 8$, vs post: $120 \pm 5\%$, $n = 7$; $p < 0.001$; AD4: pre: $146 \pm 8\%$, $n = 4$; vs post: $134 \pm 4\%$, $n = 4$; $p < 0.01$; AD5: pre: $143 \pm 8\%$, $n = 5$; vs post: $123 \pm 6\%$, $n = 5$; $p < 0.001$; AD6: pre: $153 \pm 9\%$, $n = 5$; vs post: $132 \pm 8\%$, $n = 5$; $p < 0.001$) (Fig. 4C–F). A meta-analysis of all of the multiple preincubation and postincubation samples we ran on the six AD brains showed that the preincubation samples allowed a mean 48% potentiation of baseline EPSP slope, whereas the postincubation samples allowed a mean potentiation of only 29% of baseline ($p < 0.01$). Furthermore, we found that this effect on LTP depended on the presence of Aβ because immunodepletion of Aβ rescued LTP impairment (data not shown). We conclude that

the inhibition of hippocampal synaptic plasticity conferred by smaller oligomers is significantly greater than when the oligomers from the same brain samples were in HMW aggregates.

Paired-pulse facilitation can help reveal whether alterations of synaptic transmission are principally presynaptic. In our previous work (Li et al., 2009), we used a paired-pulse facilitation paradigm with 2 rounds of stimulation and assessed whether soluble oAβ affected presynaptic release probability. Those experiments indicated that soluble oAβ in whole AD-TBS extracts did not materially alter presynaptic release probability. Similar experiments performed here showed that there was no alteration of paired-pulse facilitation by the postincubation sample of AD brain; in addition, input/output curves for both preincubation and postincubation samples did not differ (data not shown).

Postincubation LMW, but not fresh HMW, oAβ decreases neuronal levels of β-adrenergic receptors

Previous studies reported decreases in the levels of β-adrenergic receptors (βAR) and norepinephrine in several regions of AD brain (Marien et al., 2004; Szot et al., 2006; Manaye et al., 2013). Moreover, human oAβ applied to rat prefrontal cortex neurons and mouse hippocampal slices has been shown to induce internalization and degradation of βAR (Wang et al., 2011; Li et al., 2013). Indeed, we previously reported that, among 8 different monoamine neurotransmitter receptor classes quantified on cultured wt primary neurons, $β_2AR$ was the most sensitive to contact with human oAβ (Li et al., 2013). We therefore examined $β_2AR$ protein levels in hippocampal slices exposed to 2 d-incubated SEC void volume fractions versus freshly isolated void volume fractions produced by a separate SEC of the same starting AD-TBS extract. After a 4 h exposure, the levels of $β_2AR$ were decreased significantly by the postincubation sample compared with aCSF alone. They were also decreased by treatment with 10 nM of synthetic $Aβ40(S26C)_2$ dimers, which we previously found to lower $β_2AR$ expression (Li et al., 2013). Quantification documented 65% and 38% decreases in $β_2AR$, respectively, upon treating the slices with a 10 nM solution of synthetic (S26C)2 or a 20% solution of the human postincubation void volume sample in aCSF (Fig. 5). In contrast, the preincubation samples caused no change (Fig. 5). These differences indicate significantly more reduction of $β_2AR$ levels by the 2 d-incubated SEC void volume that contained small oligomers versus the preincubation samples that contained only HMW oAβ.

Small, but not large, soluble Aβ oligomers stimulate an endogenous microglial response in vivo

To establish the relative bioactivity of the preincubation and postincubation human samples in vivo, we delivered the two types of Aβ preparations into healthy, wild-type adult mice by intracerebroventricular microinjection. The preincubation and postincubation samples were again prepared from the same AD-TBS extracts. Mice were killed 48 h after the ipsilateral intracerebroventricular injection, and the contralateral hippocampal/ perihippocampal region was harvested to quantify microglial alteration by immunohistochemical morphology (Fig. 6).

We applied an unbiased microglial morphology method established previously in our laboratory for automated quantification of microglial circularity ($4\pi \times [area]/[perimeter]^2$, with 1.0 indicating a perfect circle), solidity ([area]/[convex area], with a maximum value of 1.0), number of branches/microglia, and %CD68/microglia (Xu et al., 2016). Among these four measurements, circularity and solidity describe relative cellular morphology in reference to a perfect circle or convex shape. Microglia
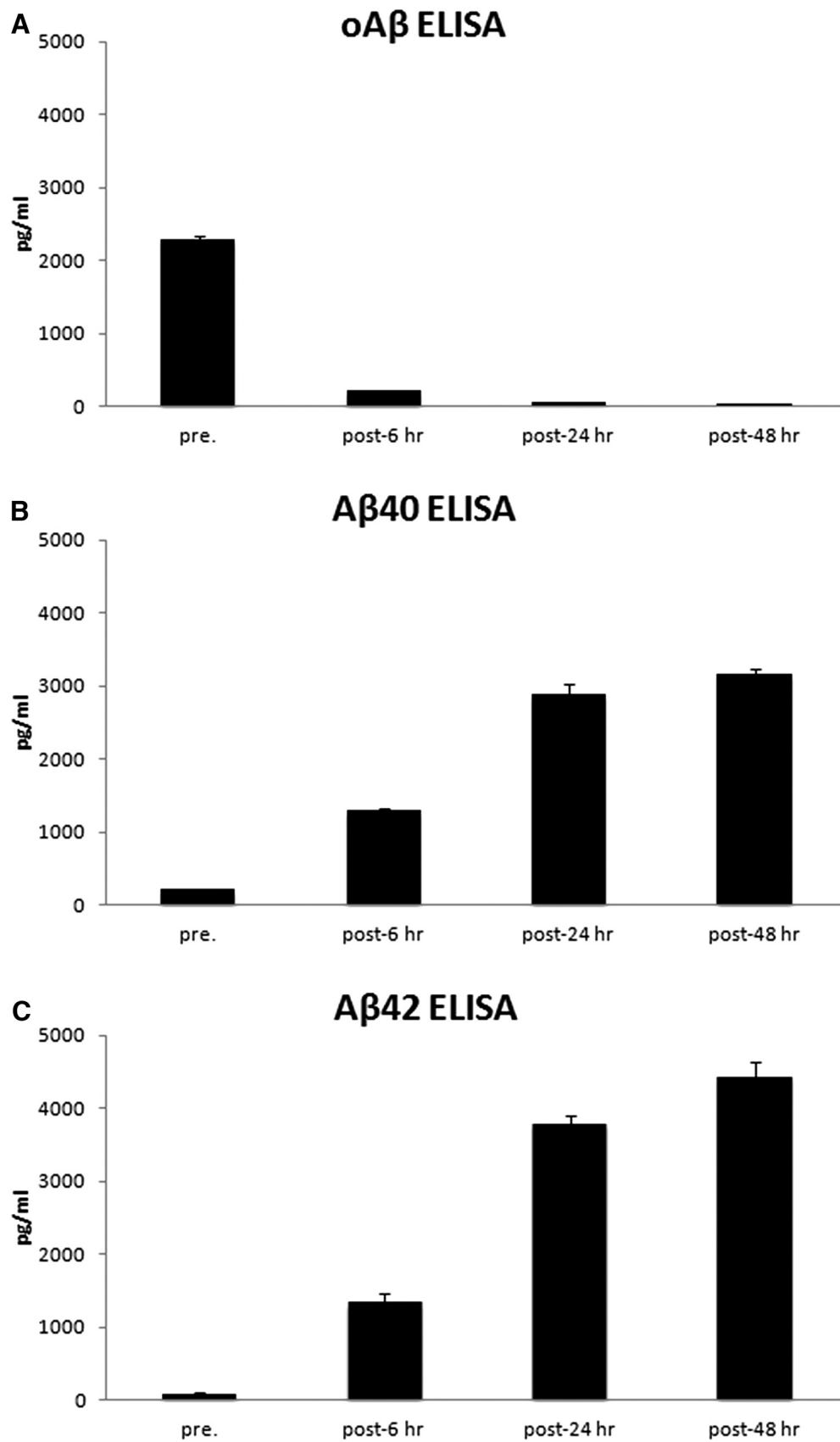
Figure 3. ELISA analyses revealed the time-dependent dissociation of void volume oAβ from AD brain. Aliquots (300 μl) of the SEC void volume fraction (fraction 6) of AD2 extract were incubated at 37°C for 0, 6, 24, or 48 h and then snap frozen in liquid nitrogen and stored at −80°C pending analysis. Samples were thawed on ice and analyzed using the oligomer-preferring (**A**) or the monomer-preferring Aβx-40 (**B**) and Aβx-42 (**C**) immunoassays.
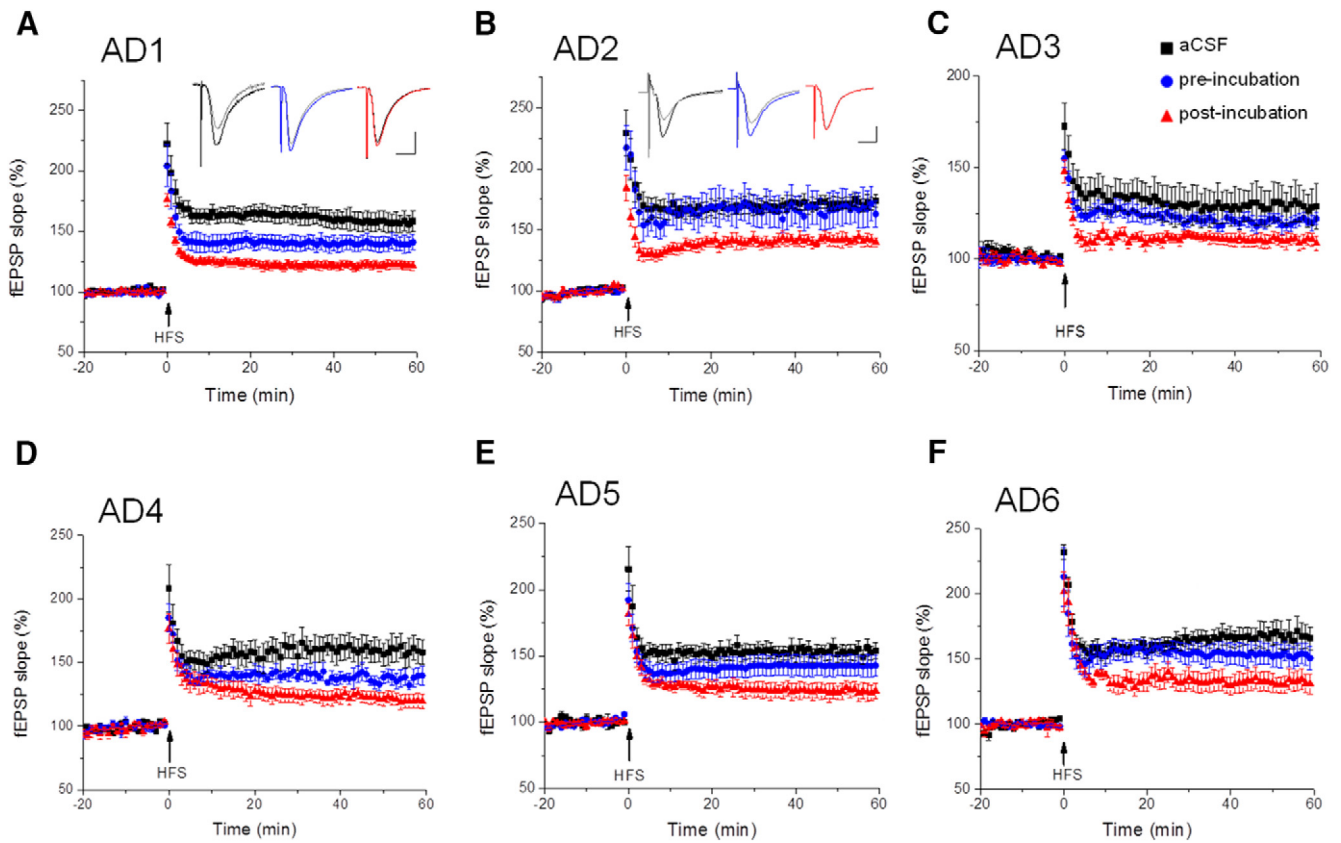
Figure 4. Incubation of HMW oAβ releases Aβ species that can inhibit hippocampal LTP. SEC void volume fractions from AD1–AD6 (**A–F**) were each tested for their effect on hippocampal LTP before *in vitro* incubation (blue circles, *n* = 8) or after incubation at 37°C for 2 d (red triangles, *n* = 10). LTP values in the text are the EPSP slopes relative to baseline just before HFS (100%) measured 60 min after a high-frequency stimulus (HFS, arrows). Two-tailed Student's *t* test and one-way ANOVA were used to determine statistical significance.
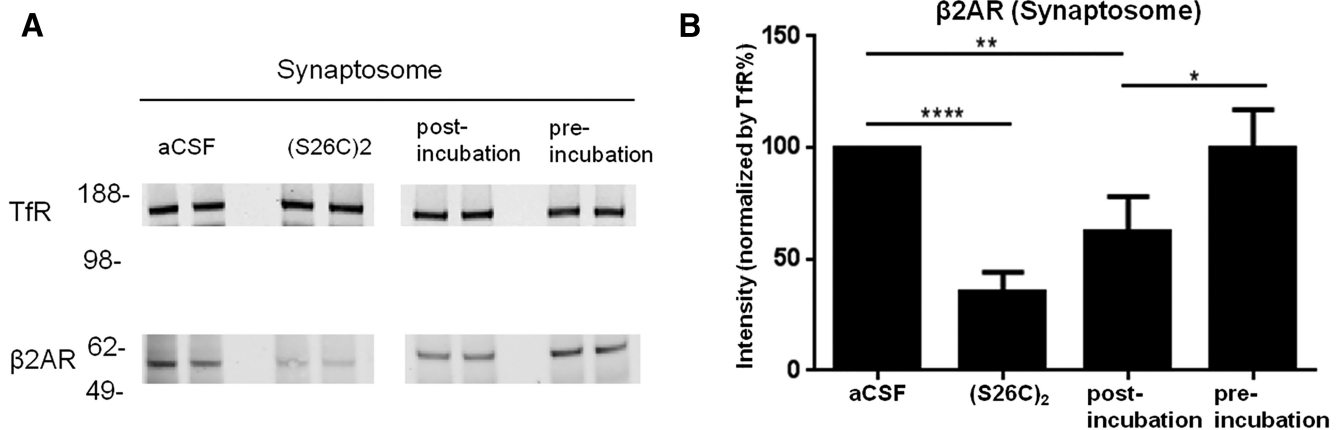

Figure 5. Incubation of HMW oAβ releases Aβ species that decrease hippocampal β₂AR levels. Hippocampal slices were exposed for 4 h to fresh or 2 d-incubated SEC void volume fractions of brain AD2, or aCSF, or 10 nM of synthetic human Aβ(S26C)₂ dimers. **A**, Hippocampal synaptosomes were then prepared and β₂AR levels quantified by Western blot and the values normalized to transferrin receptor (TfR) protein measured in the same sample. **B**, Summary data from 4 separate Western blots, as exemplified in **A**. Protein levels are normalized based on detection of TfR. Error bars indicate SEM. *$p < 0.05$; **$p < 0.01$; ****$p < 0.0001$.

with a more ramified morphology resemble a perfect circle or convex shape less than do microglia with an amoeboid morphology; thus, the former have lower circularity and solidity values. Number of branches/microglia measures the complexity of processes by quantifying total branching points. %CD68 evaluates the level of a lysosomal marker within microglia, which reflects microglial phagocytic activity. Microglia were immunostained with a recently discovered mAb to the microglia-specific surface protein P2ry12 (Butovsky et al., 2014). We observed consistent

and statistically significant differences in all four measures of microglial morphology in both the cornu ammonis (CA) and dentate gyrus (DG) of hippocampus between mice receiving the preincubation and postincubation samples of the SEC void volume fraction of AD-TBS. Mice receiving the postincubation samples had highly significant increases in contralateral microglial activation (Fig. 6), as shown by higher circularity values (CA: pre = 0.099 ± 0.013 vs post = 0.170 ± 0.026, $p < 0.0001$; DG: pre = 0.099 ± 0.012 vs post = 0.160 ± 0.022, $p < 0.0001$), higher
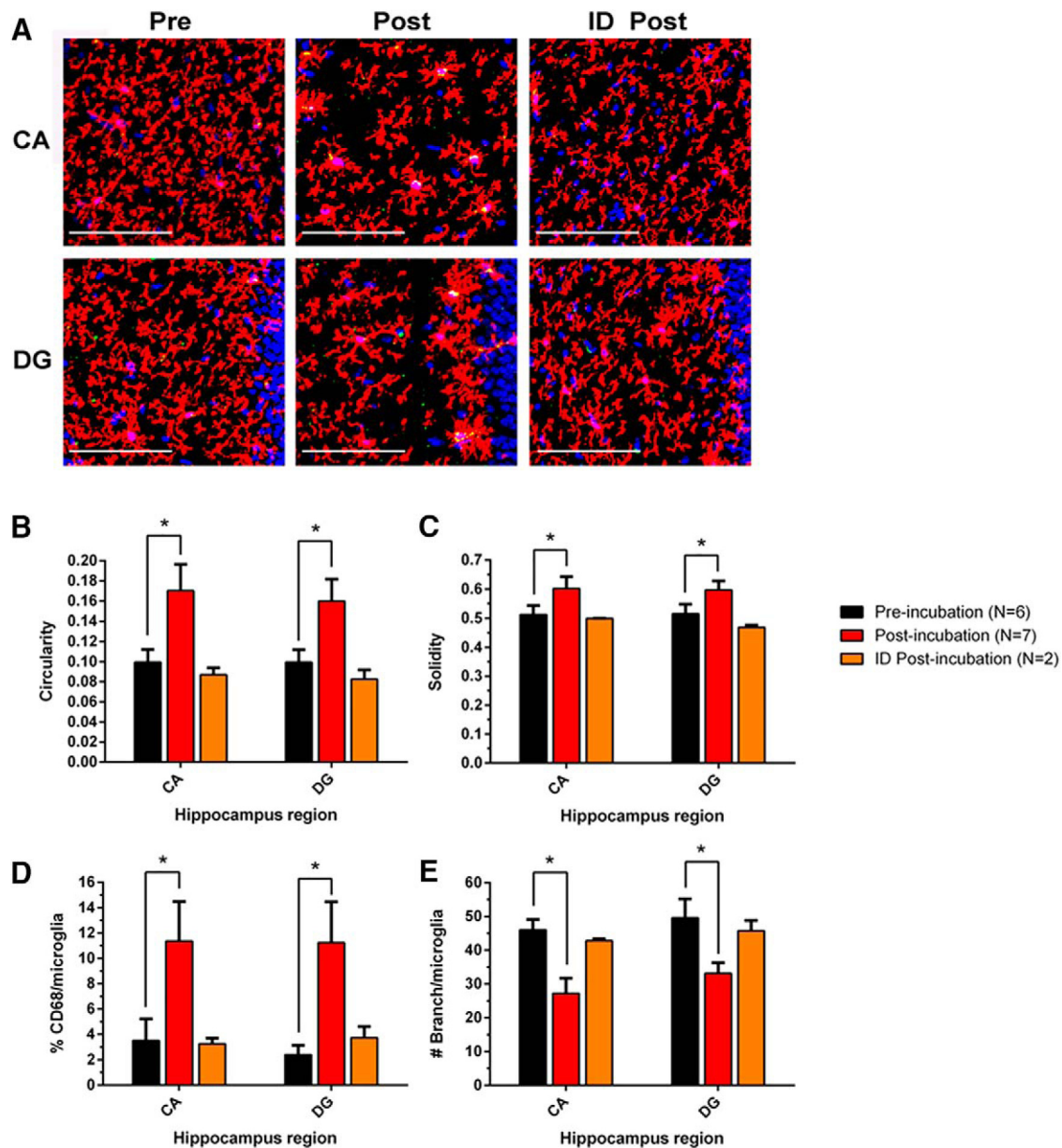
Figure 6. Incubation of HMW oAβ releases Aβ species that enhance the activation of hippocampal microglia *in vivo*. The incubated SEC void volume fraction from brain AD1 induced morphological changes in contralateral hippocampal microglia 48 h after injection into lateral ventricle. *A*, Microglial alterations were analyzed by immunohistochemical morphometry. *B*, The microglia were analyzed by unbiased automated quantification of the following: *B*, circularity ($4\pi \times$ [area]/[perimeter]^2, with 1.0 indicating a perfect circle); *C*, solidity ([area]/[convex area], with a maximum value of 1.0); (*D*) %CD68/microglia; and (*E*) no. of branches/microglia. Preincubation (black, $n = 6$), postincubation (red, $n = 7$), and ID postincubation (orange, $n = 2$) samples were microinjected into wild-type adult mice. Asterisk (*) indicates statistically significant differences; p values provided in the text.

solidity values (CA: pre $= 0.512 \pm 0.032$ vs post $= 0.602 \pm 0.042$, $p < 0.01$; DG: pre $= 0.515 \pm 0.033$ vs post $= 0.597 \pm 0.031$, $p < 0.001$), lower number of branches/microglia (CA: pre $= 46.0 \pm 3.1$ vs post $= 27.2 \pm 4.5$, $p < 0.0001$; DG: pre $= 49.6 \pm 5.6$ vs post $= 33.2 \pm 3.2$, $p < 0.0001$), and higher %CD68/microglia (CA: pre $= 3.51 \pm 1.72$ vs post $= 11.37 \pm 3.11$, $p < 0.001$; DG: pre $= 2.39 \pm 0.75$ vs post $= 11.24 \pm 3.22$, $p < 0.0001$).

To confirm that this more activated microglial morphology resulted from the small oligomeric Aβ species in the postincubation samples, we quantitatively immunodepleted Aβ from samples using the anti-Aβ mAb, 4G8 (Fig. 7), and then microinjected the immunodepleted postincubation sample (ID-post) into mice. ID-post induced significantly less intense microglial activation than the same postincubation sample before Aβ depletion,

with all measurements now statistically indistinguishable from that of the preincubation sample, indicating that the oAβ species were specifically responsible for the effects (Fig. 6).

Discussion

We and others previously reported that water-soluble extracts of AD brain potently inhibit LTP, alter synaptic form and number, and most importantly, can actually impair memory consolidation in healthy animals *in vivo* (Shankar et al., 2008; Barry et al., 2011; Freir et al., 2011; Jin et al., 2011; Li et al., 2011; Borlikova et al., 2013; Hu et al., 2014; Klyubin et al., 2014). In all cases, these effects were reversed when Aβ was removed (Shankar et al., 2008; Barry et al., 2011; Freir et al., 2011; Jin et al., 2011; Li et al., 2011; Borlikova et al., 2013; Hu
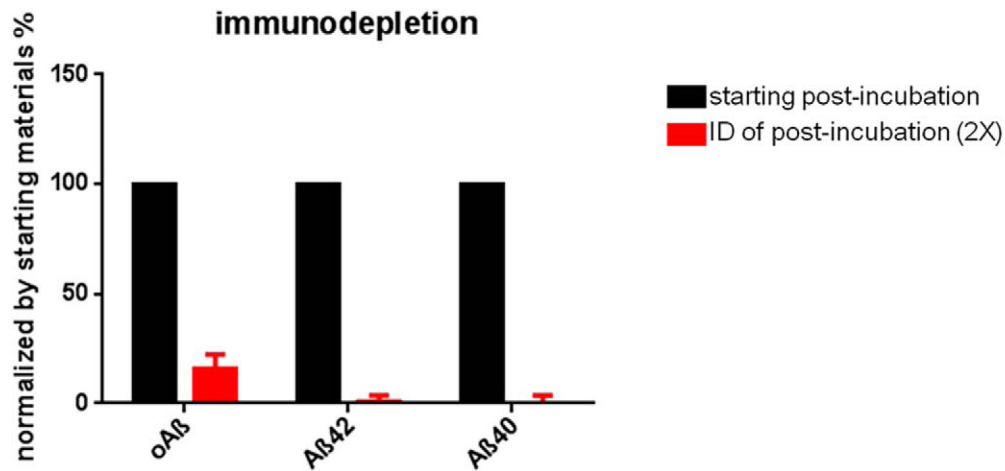
Figure 7. Anti-Aβ antibody, 4G8, quantitatively immunodepletes the void volume fractions of Aβ. SEC void volume fractions (fraction 6) of AD brain underwent 2 rounds of immunodepletion with the anti-Aβ mAb 4G8. The untreated void volume sample (black bars) and the immunodepleted sample (red bars) were then analyzed using immunoassays for oAβ, Aβx402, and Aβx-40. 4G8 treatment reduced oligomer levels by 84% and monomer levels by 99%.

et al., 2014; Klyubin et al., 2014). Many different oligomeric Aβ species have been described (Walsh and Selkoe, 2004), and there is as yet no consensus about which sized species exist, and can confer cytotoxicity, in the human brain. Immunotherapy with antibodies able to neutralize the toxicity of oligomeric Aβ species is proposed as a chronic therapy for AD (Klyubin et al., 2005; Haass and Selkoe, 2007; Walsh and Selkoe, 2007; Lord et al., 2009; Lannfelt et al., 2014; Sevigny et al., 2016), and therefore it is important for improved antibody-target selection to distinguish between diffusible Aβ species that are highly bioactive in AD brain and those that are not.

In this study, we used native SEC to separate natural oAβ aggregates of large versus small size in buffer-soluble extracts of cerebral cortex from clinically and neuropathologically typical late-onset AD patients. Our SEC results indicate that HMW oAβ assemblies comprise the vast majority of soluble Aβ species detectable in aqueous extracts of AD brain. These results are consistent with our prior studies in which we found that Aβ species with apparent molecular weights of >70 kDa were the predominant forms of Aβ in aqueous extracts from 33 different AD brains (McDonald et al., 2015). Similarly, studies using density gradient ultracentrifugation and BN-PAGE analysis (Upadhaya et al., 2012) also reported that the majority of soluble Aβ in AD brain extracts exists as HMW assemblies.

We previously observed that immunoprecipitating soluble Aβ species from AD-TBS extracts and then denaturing the precipitates in SDS detergent and separating them by Superdex 75 SEC yields LMW oligomer/dimer-rich fractions that potently impair hippocampal synaptic plasticity, enhance tau phosphorylation at AD-relevant epitopes, and induce neuritic dystrophy in primary neurons (Shankar et al., 2008; Jin et al., 2011). This work left open what role the abundant HMW soluble Aβ assemblies play in the pathogenesis of AD neurotoxicity, whether as another bioactive form or as a reservoir for the release of LMW oligomers/dimers that are possibly the principal cytotoxins. Our new data herein strongly support the latter hypothesis. We propose that the noncytotoxic monomer pool (Li et al., 2011) and the LMW Aβ oligomers are sequestered into increasingly insoluble parenchymal deposits as AD develops and progresses presymptomatically; the HMW Aβ pool is the intermediate species between monomers and LMW oligomers on the one hand and insolu-

ble amyloid plaques on the other, and there is apparently a biochemical equilibrium among these species.

The current dynamic studies of the relative properties of HMW and LMW oAβ isolated from typical late-onset AD brains offer strong evidence for the hypothesis. With the goal of attempting to disassemble the abundant HMW Aβ species, we subjected HMW Aβ (SEC void volume fractions) to incubation at 37°C for 2 d in 50 mM ammonium acetate, pH 8.5. Western blot showed that this incubation of HMW Aβ induced its dissociation into LMW oligomers/dimers and monomers, as shown by a second SEC run that demonstrated a "shift to the right": a marked decrease in the Aβ signals in the void volume fractions and a parallel increase in the Aβ signals in dimer and monomer fractions (Fig. 2A). Our oAβ-selective immunoassay showed that void volume fractions from the first Superdex 75 run produced robust signals, but after the 2 d incubation, the oAβ signals in this first void volume fraction were dramatically decreased, whereas the monomeric Aβ signals detectable by a conventional 1-x monomer ELISA were correspondingly increased (Table 2). We confirmed this dissociation of HMW Aβ to LMW/dimeric Aβ and monomers by a second SEC run followed by ELISAs of all fractions (Fig. 2B).

Experiments using freshly isolated void volume HMW oAβ revealed that this material did not significantly alter hippocampal synaptic plasticity (Fig. 4). This does not mean that the HMW Aβ oligomers have no pathogenic role; rather, our collective experimental findings suggest that they serve as relatively inert reservoirs of small bioactive oligomers. In accord, the postincubation samples contained LMW oligomers/dimers and showed significantly greater LTP inhibition than the void volume before incubation.

The noradrenergic signaling system is known to participate in various forms of learning and memory. βAR blockade can impair attention, learning and memory in animals and humans (Cahill et al., 2000; Chamberlain et al., 2006). In AD brain tissue, decreases in the levels of βARs have been reported in several brain regions (Marien et al., 2004; Szot et al., 2006; Manaye et al., 2013), presumably due in part to the observed loss of noradrenergic neurons in the locus ceruleus (Grudzien et al., 2007; Weinshenker, 2008; Manaye et al., 2013). One plausible mechanism for the reduced βAR levels in AD brain is an oAβ-induced degradation of the receptors (Wang et al., 2011), and this is what we found

after the application of the postincubation void volume (Fig. 5). The latter, but not the freshly isolated void volume fractions, decreased β2AR levels in synaptosome fractions of wild-type mouse hippocampal slices.

In an attempt to demonstrate the relative bioactivities *in vivo* of LMW and HMW oAβ from the same human brain, we performed intracerebroventricular microinjections into normal adult wt mice. Freshly isolated HMW oAβ (preincubation) and duplicate void volume fractions isolated from the same AD TBS extract but incubated to facilitate its dissociation to LMW Aβ species (postincubation) were tested side by side. The postincubation samples induced a significantly higher degree of microglial activation in the contralateral hippocampal region. While the SEC void volume of AD-TBS contains many biomolecules that could change upon prolonged incubation and alter microglia physiology, the fact that the microglial activation was fully prevented by selective immunodepletion with an anti-Aβ monoclonal antibody indicates that the observed effects on microglia *in vivo* are mediated by LMW forms of soluble Aβ.

How do the data from our biochemical experiments relate to what may occur in the brain tissue of living AD subjects? The relevance of our study to AD derives from the fact that all of the human brain soluble extracts we analyzed came from patients dying with clinically and neuropathologically typical AD. In this initial study, we focused on available postmortem brains obtained at a late stage of clinical symptomatology. In future studies, we will seek to obtain brain tissue from humans who died at the MCI stage. But it is likely that the resultant data would be similar to our current findings because amyloid pathology (as reflected by neuropathological studies, amyloid PET imaging, and low CSF Aβ42 levels) is already highly abundant at the MCI stage and has been shown to accrue many years or even 2 decades before the appearance of early cognitive symptoms in AD (see e.g., Bateman et al., 2012; Jack and Holtzman, 2013; Villemagne et al., 2013). These and other studies indicate that, by the MCI clinical stage, Aβ accumulation is usually advanced. In accord, mean total amyloid plaque number in AD brains does not rise significantly between the earliest clinical stage and the latest (terminal) stage of symptomatic AD (Hyman et al., 1995). Moreover, in preliminary studies of aqueous extracts of brains from individuals who died at the mild AD stage (e.g., MMSE ∼24), HMW Aβ oligomers were again the most abundant Aβ species detected (T. O'Malley and D.M.W., unpublished data).

Our experiments imply that there is a dynamic equilibrium in AD brain between HMW, largely biologically inactive oAβ forms and lower MW, more bioactive forms (e.g., as found in the penumbra of fibrillar amyloid plaques). Evidence for the latter concept comes from APP tg mice, where an oligomer-selective antibody enabled imaging of a penumbra of soluble oligomers surrounding fibrillar plaques (Koffie et al., 2009). The authors showed that neurites were dystrophic and synapses depleted in this zone, but their densities became normal as one measured farther from the fibrillar plaque border. A transition from larger insoluble to smaller more diffusible oAβ species, presumably similar to those we generated by incubation of HMW soluble fractions, is likely to occur at the outer border of dense-core plaques.

Together, our results indicate that HMW oAβ are the predominant form of Aβ in the soluble fraction of AD cortex and are far less bioactive than the smaller oligomers to which they can dissociate. Based on the data herein, we hypothesize that Aβ plaques are composed of both fibrillar Aβ and soluble HMW oAβ. We speculate that LMW oAβ can be sequestered into both

soluble HMW oAβ and eventually into increasingly insoluble fibrillar deposits. The HMW oAβ we describe may thus be an intermediate species between insoluble fibrillar Aβ and the LMW oAβ that we show induces neuronal and microglial toxicity. All of these forms are likely to be in a complex equilibrium in the human brain.

References

Barry AE, Klyubin I, McDonald JM, Mably AJ, Farrell MA, Scott M, Walsh DM, Rowan MJ (2011) Alzheimer's disease brain-derived amyloid-beta-mediated inhibition of LTP in vivo is prevented by immunotargeting cellular prion protein. J Neurosci 31:7259–7263. CrossRef Medline

Bateman RJ, Xiong C, Benzinger TL, Fagan AM, Goate A, Fox NC, Marcus DS, Cairns NJ, Xie X, Blazey TM, Holtzman DM, Santacruz A, Buckles V, Oliver A, Moulder K, Aisen PS, Ghetti B, Klunk WE, McDade E, Martins RN, et al. (2012) Clinical and biomarker changes in dominantly inherited Alzheimer's disease. N Engl J Med 367:795–804. CrossRef Medline

Borlikova GG, Trejo M, Mably AJ, McDonald JM, Sala Frigerio C, Regan CM, Murphy KJ, Masliah E, Walsh DM (2013) Alzheimer brain-derived amyloid beta-protein impairs synaptic remodeling and memory consolidation. Neurobiol Aging 34:1315–1327. CrossRef Medline

Butovsky O, Jedrychowski MP, Moore CS, Cialic R, Lanser AJ, Gabriely G, Koeglsperger T, Dake B, Wu PM, Doykan CE, Fanek Z, Liu L, Chen Z, Rothstein JD, Ransohoff RM, Gygi SP, Antel JP, Weiner HL (2014) Identification of a unique TGF-beta-dependent molecular and functional signature in microglia. Nat Neurosci 17:131–143. CrossRef Medline

Cahill L, Pham CA, Setlow B (2000) Impaired memory consolidation in rats produced with beta-adrenergic blockade. Neurobiol Learn Mem 74:259–266. CrossRef Medline

Chamberlain SR, Müller U, Blackwell AD, Robbins TW, Sahakian BJ (2006) Noradrenergic modulation of working memory and emotional memory in humans. Psychopharmacology 188:397–407. CrossRef Medline

Freir DB, Nicoll AJ, Klyubin I, Panico S, McDonald JM, Risse E, Asante EA, Farrow MA, Sessions RB, Saibil HR, Clarke AR, Rowan MJ, Walsh DM, Collinge J (2011) Interaction between prion protein and toxic amyloid beta assemblies can be therapeutically targeted at multiple sites. Nat Commun 2:336. CrossRef Medline

Grudzien A, Shaw P, Weintraub S, Bigio E, Mash DC, Mesulam MM (2007) Locus coeruleus neurofibrillary degeneration in aging, mild cognitive impairment and early Alzheimer's disease. Neurobiol Aging 28:327–335. CrossRef Medline

Haass C, Selkoe DJ (2007) Soluble protein oligomers in neurodegeneration: lessons from the Alzheimer's amyloid beta-peptide. Nat Rev Mol Cell Biol 8:101–112. CrossRef Medline

Hu NW, Nicoll AJ, Zhang D, Mably AJ, O'Malley T, Purro SA, Terry C, Collinge J, Walsh DM, Rowan MJ (2014) mGlu5 receptors and cellular prion protein mediate amyloid-beta-facilitated synaptic long-term depression in vivo. Nat Commun 5:3374. CrossRef Medline

Hyman BT, West HL, Rebeck GW, Buldyrev SV, Mantegna RN, Ukleja M, Havlin S, Stanley HE (1995) Quantitative analysis of senile plaques in Alzheimer disease: observation of log-normal size distribution and molecular epidemiology of differences associated with apolipoprotein E genotype and trisomy 21 (Down syndrome). Proc Natl Acad Sci U S A 92:3586–3590. CrossRef Medline

Jack CR Jr, Holtzman DM (2013) Biomarker modeling of Alzheimer's disease. Neuron 80:1347–1358. CrossRef Medline

Jin M, Shepardson N, Yang T, Chen G, Walsh D, Selkoe DJ (2011) Soluble amyloid beta-protein dimers isolated from Alzheimer cortex directly induce Tau hyperphosphorylation and neuritic degeneration. Proc Natl Acad Sci U S A 108:5819–5824. CrossRef Medline

Klyubin I, Walsh DM, Lemere CA, Cullen WK, Shankar GM, Betts V, Spooner ET, Jiang L, Anwyl R, Selkoe DJ, Rowan MJ (2005) Amyloid beta protein immunotherapy neutralizes Abeta oligomers that disrupt synaptic plasticity in vivo. Nat Med 11:556–561. CrossRef Medline

Klyubin I, Nicoll AJ, Khalili-Shirazi A, Farmer M, Canning S, Mably A, Linehan J, Brown A, Wakeling M, Brandner S, Walsh DM, Rowan MJ, Collinge J (2014) Peripheral administration of a humanized anti-PrP antibody blocks Alzheimer's disease Abeta synaptotoxicity. J Neurosci 34:6140–6145. CrossRef Medline

Koffie RM, Meyer-Luehmann M, Hashimoto T, Adams KW, Mielke ML, Garcia-Alloza M, Micheva KD, Smith SJ, Kim ML, Lee VM, Hyman BT, Spires-Jones TL (2009) Oligomeric amyloid beta associates with post-

synaptic densities and correlates with excitatory synapse loss near senile plaques. Proc Natl Acad Sci U S A 106:4012–4017. CrossRef Medline

Lannfelt L, Möller C, Basun H, Osswald G, Sehlin D, Satlin A, Logovinsky V, Gellerfors P (2014) Perspectives on future Alzheimer therapies: amyloid-beta protofibrils: a new target for immunotherapy with BAN2401 in Alzheimer's disease. Alzheimers Res Ther 6:16. CrossRef Medline

Li S, Hong S, Shepardson NE, Walsh DM, Shankar GM, Selkoe D (2009) Soluble oligomers of amyloid beta protein facilitate hippocampal long-term depression by disrupting neuronal glutamate uptake. Neuron 62: 788–801. CrossRef Medline

Li S, Jin M, Koeglsperger T, Shepardson NE, Shankar GM, Selkoe DJ (2011) Soluble Abeta oligomers inhibit long-term potentiation through a mechanism involving excessive activation of extrasynaptic NR2B-containing NMDA receptors. J Neurosci 31:6627–6638. CrossRef Medline

Li S, Jin M, Zhang D, Yang T, Koeglsperger T, Fu H, Selkoe DJ (2013) Environmental novelty activates beta2-adrenergic signaling to prevent the impairment of hippocampal LTP by Abeta oligomers. Neuron 77:929–941. CrossRef Medline

Lord A, Gumucio A, Englund H, Sehlin D, Sundquist VS, Söderberg L, Moller C, Gellerfors P, Lannfelt L, Pettersson FE, Nilsson LN (2009) An amyloid-beta protofibril-selective antibody prevents amyloid formation in a mouse model of Alzheimer's disease. Neurobiol Dis 36:425–434. CrossRef Medline

Mably AJ, Liu W, McDonald JM, Dodart JC, Bard F, Lemere CA, O'Nuallain B, Walsh DM (2015) Anti-Abeta antibodies incapable of reducing cerebral Abeta oligomers fail to attenuate spatial reference memory deficits in J20 mice. Neurobiol Dis 82:372–384. CrossRef Medline

Manaye KF, Mouton PR, Xu G, Drew A, Lei DL, Sharma Y, Rebeck GW, Turner S (2013) Age-related loss of noradrenergic neurons in the brains of triple transgenic mice. Age 35:139–147. CrossRef Medline

Marien MR, Colpaert FC, Rosenquist AC (2004) Noradrenergic mechanisms in neurodegenerative diseases: a theory. Brain Res Brain Res Rev 45:38–78. CrossRef Medline

McDonald JM, O'Malley TT, Liu W, Mably AJ, Brinkmalm G, Portelius E, Wittbold WM 3rd, Frosch MP, Walsh DM (2015) The aqueous phase of Alzheimer's disease brain contains assemblies built from approximately 4 and approximately 7 kDa Abeta species. Alzheimers Dement 11:1286–1305. CrossRef Medline

O'Malley TT, Oktaviani NA, Zhang D, Lomakin A, O'Nuallain B, Linse S, Benedek GB, Rowan MJ, Mulder FA, Walsh DM (2014) Abeta dimers differ from monomers in structural propensity, aggregation paths and population of synaptotoxic assemblies. Biochem J 461:413–426. CrossRef Medline

O'Nuallain B, Freir DB, Nicoll AJ, Risse E, Ferguson N, Herron CE, Collinge J, Walsh DM (2010) Amyloid beta-protein dimers rapidly form stable synaptotoxic protofibrils. J Neurosci 30:14411–14419. CrossRef Medline

Sevigny J, Chiao P, Bussière T, Weinreb PH, Williams L, Maier M, Dunstan R, Salloway S, Chen T, Ling Y, O'Gorman J, Qian F, Arastu M, Li M, Chollate S, Brennan MS, Quintero-Monzon O, Scannevin RH, Arnold HM, Engber T, et al. (2016) The antibody aducanumab reduces Abeta plaques in Alzheimer's disease. Nature 537:50–56. CrossRef Medline

Shankar GM, Li S, Mehta TH, Garcia-Munoz A, Shepardson NE, Smith I, Brett FM, Farrell MA, Rowan MJ, Lemere CA, Regan CM, Walsh DM, Sabatini BL, Selkoe DJ (2008) Amyloid-beta protein dimers isolated directly from Alzheimer's brains impair synaptic plasticity and memory. Nat Med 14:837–842. CrossRef Medline

Shankar GM, Welzel AT, McDonald JM, Selkoe DJ, Walsh DM (2011) Isolation of low-n amyloid beta-protein oligomers from cultured cells, CSF, and brain. Methods Mol Biol 670:33–44. CrossRef Medline

Szot P, White SS, Greenup JL, Leverenz JB, Peskind ER, Raskind MA (2006) Compensatory changes in the noradrenergic nervous system in the locus ceruleus and hippocampus of postmortem subjects with Alzheimer's disease and dementia with Lewy bodies. J Neurosci 26:467–478. CrossRef Medline

Upadhaya AR, Lungrin I, Yamaguchi H, Fändrich M, Thal DR (2012) High-molecular weight Abeta oligomers and protofibrils are the predominant Abeta species in the native soluble protein fraction of the AD brain. J Cell Mol Med 16:287–295. CrossRef Medline

Villemagne VL, Burnham S, Bourgeat P, Brown B, Ellis KA, Salvado O, Szoeke C, Macaulay SL, Martins R, Maruff P, Ames D, Rowe CC, Masters CL, Masters CL (2013) Amyloid beta deposition, neurodegeneration, and cognitive decline in sporadic Alzheimer's disease: a prospective cohort study. Lancet Neurol 12:357–367. CrossRef Medline

Walsh DM, Selkoe DJ (2004) Oligomers on the brain: the emerging role of soluble protein aggregates in neurodegeneration. Protein Pept Lett 11: 213–228. CrossRef Medline

Walsh DM, Selkoe DJ (2007) Abeta oligomers: a decade of discovery. J Neurochem 101:1172–1184. CrossRef Medline

Wang D, Yuen EY, Zhou Y, Yan Z, Xiang YK (2011) Amyloid beta peptide-(1–42) induces internalization and degradation of beta2 adrenergic receptors in prefrontal cortical neurons. J Biol Chem 286:31852–31863. CrossRef Medline

Weinshenker D (2008) Functional consequences of locus coeruleus degeneration in Alzheimer's disease. Curr Alzheimer Res 5:342–345. CrossRef Medline

Xia W, Yang T, Shankar G, Smith IM, She, Y, Walsh DM, Dennis J, Selkoe M (2009) A specific enzyme-linked immunosorbent assay for measuring β-amyloid protein oligomers in human plasma and brain tissue of patients with Alzheimer disease. Arch Neurol 66:190–199. CrossRef Medline

Xu H, Gelyana E, Rajsombath M, Yang T, Li S, Selkoe D (2016) Environmental enrichment potently prevents microglia-mediated neuroinflammation by human amyloid beta-protein oligomers. J Neurosci 36: 9041–9056. CrossRef Medline

Yang T, Hong S, O'Malley T, Sperling RA, Walsh DM, Selkoe DJ (2013) New ELISAs with high specificity for soluble oligomers of amyloid beta-protein detect natural Abeta oligomers in human brain but not CSF. Alzheimers Dement 9:99–112. CrossRef Medline

Yang T, O'Malley TT, Kanmert D, Jerecic J, Zieske LR, Zetterberg H, Hyman BT, Walsh DM, Selkoe DJ (2015) A highly sensitive novel immunoassay specifically detects low levels of soluble Abeta oligomers in human cerebrospinal fluid. Alzheimers Res Ther 7:14. CrossRef Medline